NACA

RESEARCH MEMORANDUM

EXPERIMENTAL INVESTIGATION OF TURBINE STATOR-BLADE-

OUTLET BOUNDARY-LAYER CHARACTERISTICS AND A

COMPARISON WITH THEORETICAL RESULTS

By Warren J. Whitney, Warner L. Stewart, and James W. Miser

Lewis Flight Propulsion Laboratory
Cleveland, Ohio

CLASSIFICATION CHANGED

To _____ UNCLASSIFIED

By authority of ___ *RN-116* _____ Date _____

NACA Rec abu

GL 7-8-57

NATIONAL ADVISORY COMMITTEE
FOR AERONAUTICS
WASHINGTON
March 16, 1956

NATIONAL ADVISORY COMMITTEE FOR AERONAUTICS

RESEARCH MEMORANDUM

EXPERIMENTAL INVESTIGATION OF TURBINE STATOR-BLADE-OUTLET BOUNDARY-

LAYER CHARACTERISTICS AND A COMPARISON WITH THEORETICAL RESULTS

By Warren J. Whitney, Warner L. Stewart, and James W. Miser

SUMMARY

The boundary-layer characteristics at the mean radius immediately downstream of a typical turbine stator blade have been investigated experimentally over a range of blade-outlet critical-velocity ratio from 0.8 to 1.16. The total boundary-layer momentum thickness for the blade and the individual thicknesses obtained for the suction and pressure surfaces are compared with the values calculated from the turbulent-boundary-layer theory. In addition, the boundary-layer form factors, pressure factors, and energy factors obtained in the investigation for the blade and for the two surfaces individually are compared herein with those obtained from a simple-power-law velocity profile having an exponent of 1/7.

The theoretical values of boundary-layer momentum thickness were in reasonably close agreement with the experimental values, the theoretical values being slightly lower over the range of critical-velocity ratio. The trend of the theoretical curve of momentum thickness as a function of critical-velocity ratio was similar to that of the experimental results. This fact verified to some extent the effect of Reynolds and Mach numbers that was assumed in the theoretical method. The blade-outlet boundary-layer form factors, pressure factors, and energy factors for the blade and for the two surfaces could be satisfactorily approximated by a simple-power-law velocity profile having an exponent of 1/7.

INTRODUCTION

One of the prime objectives of the turbine research program being conducted at the NACA Lewis laboratory is a better understanding of the fundamental nature of the flow and the sources of loss encountered in turbomachine blade rows. An understanding of this type would enable the designer to use sound aerodynamic concepts, rather than empirical guides, for selecting such pertinent design features as turning angle, relative Mach number, solidity, and reaction for a given blading design. A reasonably accurate estimate of the blade-outlet boundary-layer

characteristics, for instance, would serve as a basis for predetermin-
ing the mass-flow and loss coefficients for a blading design.

The boundary-layer characteristics of airfoils at low Mach numbers
have been investigated in the past, and a considerable amount of this
low-speed data is available (e.g., refs. 1 and 2). Little high-speed
data is available, however, and not much work has been done toward pre-
dicting boundary-layer characteristics for blading in the field of high
flow velocities where the incompressible-flow solutions are inadequate.
In reference 3 the basic boundary-layer parameters are described for
compressible flow in terms of conventional nondimensional flow param-
eters. It is shown in reference 3 that compressibility has considerable
effect on the pressure parameter and pressure loss in the boundary layer
at high velocities. It is also shown (ref. 3) that blade losses depend
primarily on the boundary-layer momentum thickness.

Therefore, it was of interest to determine experimentally the
blade-outlet boundary-layer characteristics for a typical turbine stator-
blade row in the compressible-flow velocity range. Total-pressure sur-
veys were made at the mean radius immediately downstream of the stator-
blade trailing edge over a range of critical-velocity ratio from 0.8 to
1.4. The boundary-layer parameters were calculated by integrating mass
flow and velocity from the total-pressure profiles. This report pre-
sents the boundary-layer characteristics obtained from the surveys. In
addition, the boundary-layer momentum thicknesses are compared to those
calculated from turbulent-boundary-layer theory.

APPARATUS AND PROCEDURE

The test installation consisted of an annular cascade of turbine
stator blades with the turbine rotor removed. The stator blading used
in this investigation was a typical free-vortex straight-back design
having a turning angle of 62° at the mean radius. The tip diameter was
14 inches and the hub-tip radius ratio was 0.7. The mean radius pitch
was 1.168 inches and the chord length was 2.068 inches. A sketch show-
ing the stator-blade passages and profiles is shown in figure 1. Sur-
veys were made at various outlet static pressures to cover a range of
critical-velocity ratio from 0.8 to 1.4. The upstream total tempera-
ture and pressure were maintained constant at nominal values of 600° R
and 32 inches of mercury absolute. The survey probe was located axially
so that the sensing element just cleared the blade trailing edge by a
few thousandths of an inch.

The surveys consisted of circumferential traverses at the mean
radius made by a total-pressure probe aligned with the flow angle. The
hook-type total-pressure probe was made from a single 0.020-inch tube
flattened to a width of 0.006 inch in the tangential direction.

The pressure impulse sensed by the probe was converted to milli-volts and this signal was plotted as a continuous function of probe position on an automatic curve tracer. The trace readings reduced to total pressures by instrument calibration were used to integrate the mass flow, total pressure, kinetic energy, and momentum through the boundary layer. The static pressure was assumed constant along the circumferential path and was obtained by averaging the values obtained at the inner and outer shrouds. The inner- and outer-shroud static pressures were based on the average pressure obtained from four static-pressure taps located in the centers of stator passages spaced 90° apart on the shrouds.

CALCULATIONS

Experimental Boundary-Layer Characteristics

The total-pressure traces are shown in figure 2 for the various blade-outlet critical-velocity ratios. The blade over-all boundary-layer parameters, δ^*_{tot}, θ^*_{tot}, ξ^*_{tot}, and ψ^*_{tot} (all symbols are defined in appendix A), were obtained for these experimental data by integrating the velocity, mass flow, and total pressure along a circumferential path across one blade pitch using equations (17) of reference 3. In obtaining δ^*_{tot}, the trailing-edge thickness term δ_{te} was omitted from the equation because there was no perceptible mass-flow-void part of the wake region corresponding to the trailing-edge blockage (fig. 2). Although the probe was as close as possible to the trailing edge, the rounded trailing-edge shape would permit the boundary-layer fluids to flow into the trailing-edge region. The ratio of total momentum thickness to chord was obtained from

$$\frac{\theta_{tot}}{c} = \frac{\theta^*_{tot} \; s \; \cos \beta}{c} \tag{1}$$

The parameters H_{tot}, P_{tot}, and E_{tot} were obtained from δ^*_{tot}, θ^*_{tot}, ξ^*_{tot}, and ψ^*_{tot}. In order to obtain these quantities for the two surfaces individually, a demarcation point D between the suction- and pressure-surface boundary-layer regions was arbitrarily selected as the minimum total-pressure point (fig. 2). The suction-surface parameters θ^*_s, δ^*_s, ξ^*_s, and ψ^*_s were obtained by integrating the same equations (eqs. (17) of ref. 3) from $u/s = 0$ to $u/s = d/s$. The pressure-surface parameters were then obtained from $\theta^*_{tot} = \theta^*_s + \theta^*_p$ and corresponding equations for δ^*_{tot}, ξ^*_{tot}, and ψ^*_{tot}. The parameters H, P, and E for the two surfaces could then be calculated from these quantities since

$$H_s = \frac{\delta_s^*}{\theta_s^*} \tag{2a}$$

and

$$H_p = \frac{\delta_p^*}{\theta_p^*} \tag{2b}$$

For higher supersonic blade-outlet velocities, the indicated free-stream total pressure was lower than the inlet total pressure (fig. 2). This effect is most noticeable at the two highest blade-outlet velocities $((V/V_{cr})_{0,2} = 1.24$ and $1.40)$. There are two possible reasons for the blade-outlet free-stream total pressure being lower than the inlet total pressure at these velocity levels. First, there could have been a shock pattern in the blade row downstream of the throat section. The shocks would have extended across the free-stream flow and lowered the free-stream total pressure. Second, the pressure indicated by the probe could have been in error because of a detached bow wave ahead of the probe sensing element. Applying a normal-shock-loss correction to the indicated total pressure resulted in an outlet free-stream total pressure that was greater than the inlet total pressure. The loss in free-stream total pressure was probably due to a combination of the two reasons given. If any significant loss occurred in the free-stream flow, the development of reference 3 is not valid; and the evaluation of the boundary-layer characteristics would become extremely complex, even if the true total-pressure profile at the blade outlet were known. Therefore, no attempt was made to evaluate the boundary-layer characteristics at the two highest blade-outlet velocities because it was believed that the accuracy of these quantities would be highly questionable and, therefore, of little value.

Theoretical Boundary-Layer Characteristics

The boundary-layer form factor H, energy factor E, and pressure factor P can be computed for a simple-power-law velocity profile. These three factors are functions of the blade-outlet critical-velocity ratio $(V/V_{cr})_{0,2}$ and the simple-power-law-velocity-profile exponent n. The theoretical values of H, P, and E were computed for $n = 1/7$ by using equations (B12), (B13), and (B14) of reference 3. The quantities H, P, and E are independent of the physical boundary-layer thickness; however, they do serve to indicate whether the boundary-layer properties can be approximated by a simple-power-law velocity profile.

Momentum Thickness Obtained from Turbulent-Boundary-Layer Theory

In order to calculate the theoretical values of the boundary-
layer thickness, it was necessary to estimate the velocity distribution
around the blade by applying the stream-filament theory (ref. 4) to the
blade mean section. The velocity distributions were determined for
blade-outlet critical-velocity ratios of 0.5, 0.75, 1.00, and 1.46
(limiting loading). For the case of stator limiting loading, the
suction-surface velocity downstream of the throat was obtained by the
method of characteristics with no shock losses assumed. Isentropic
flow through the stator was assumed in all cases. The velocity dis-
tributions are shown in figure 3. The turbulent-boundary-layer thick-
nesses were computed by using the following relations:

$$\tau \, dx = \frac{d(\rho_0 V_0^2 \theta)}{g} + \frac{\rho_0 V_0 \delta}{g} \, dV_0 \tag{3}$$

$$\tau = \frac{C_{fr,inc} \rho_0 V_0^2}{2g} = \left(\frac{\rho_0 V_0^2}{2g}\right)\left(\frac{0.246}{Re_\theta^{0.268} \, 10^{0.678 H_{inc}}}\right) \tag{4}$$

Equation (3) is the Kármán momentum equation of reference 5. Equation
(4) is an empirical equation for the wall shearing stress from refer-
ence 6. Since this relation was developed for incompressible flow, the
substitution $H_{inc} = (2n + 1)$ is used herein (ref. 3). This substitu-
tion assumes, in effect, that the boundary layer has a simple-power-
law velocity profile. Reference 7 shows that compressibility has an
effect on wall shearing stress and skin-friction coefficient. The
correlating relation is given by

$$C_{fr,inc} = C_{fr,c} \, K \tag{5}$$

where

$$K = \left[1 - \frac{\gamma - 1}{\gamma + 1}\left(\frac{V}{V_{cr}}\right)_0^2\right]^{0.467}$$

The factor K was included in the empirical shearing-stress equation.
When this relation was substituted in the momentum equation (eq. (3)),
the resulting equation (appendix B) was integrable as follows:

$$\theta_x =$$

$$\frac{0.231}{\left[\left(\frac{\rho V}{\rho' V_{cr}}\right)_0 \left(\frac{V}{V_{cr}}\right)_0^{(1+H)}\right]_x} \left\{\int_0^x \frac{\left[\left(\frac{\rho V}{\rho' V_{cr}}\right)_0 \left(\frac{V}{V_{cr}}\right)_0^{(1+H)}\right]^{1.268} \left(\frac{\mu}{\rho V}\right)_0^{0.268} K \, dx}{10^{0.678(2n+1)}}\right\}^{0.7886}$$

(6)

The form factor H is the compressible-flow form factor. In order to complete the solution for θ_x, it was necessary to estimate the values of H and n by an approximate method. The exponent n was obtained from the equation

$$1/n = 2.6 \, Re_{0,x}^{1/14}$$

(7)

from reference 8, where $Re_{0,x}$ is the free-stream Reynolds number based on surface length at any particular point. The value of H could then be determined from table III of reference 8, from the critical-velocity ratio and the value of $1/n$. The use of this relation between n and H assumes in effect that the boundary layer has a simple-power-law velocity profile. The value of θ was obtained by graphically integrating the right-hand side of equation (6).

It has been assumed, herein, that the flow at the mean radius section is essentially two-dimensional, or that there is no appreciable radial flow of the boundary-layer fluids. This assumption was substantiated to some extent by a low-speed smoke-flow test that was made on this blade channel. In the low-speed visual flow test there was no perceptible radial transfer of the boundary-layer fluids. It was believed that the transition from a laminar to a turbulent boundary layer occurred early on the blade surfaces because of the high inlet turbulence intensity, which was measured as 7 percent. In calculations of the theoretical values of boundary-layer momentum thickness, the boundary layer was assumed turbulent from the forward stagnation point.

RESULTS AND DISCUSSION

The boundary-layer characteristics occurring at the mean section of the stator blade were obtained from the experimental information in the manner described in the CALCULATIONS section. This information included the blade over-all characteristics as well as the characteristics occurring on each surface.

3949

Over-All Characteristics

Momentum loss. - In figure 4 the ratio of total momentum thickness to chord $(\theta_{tot}/c)_2$ is presented as a function of the blade-outlet critical-velocity ratio $(V/V_{cr})_{0,2}$. The values of $(\theta_{tot}/c)_2$ decreased as the velocity increased. This trend is believed to result largely from the Reynolds and Mach number effects on the skin-friction coefficient as is discussed later in this section.

Form and loss factors. - The three boundary-layer factors H_{tot}, E_{tot}, and P_{tot} were also obtained over the range of velocities covered in this investigation. These factors are related to the momentum thickness parameter θ and are measures of flow blockage, kinetic-energy loss, and total-pressure loss, respectively (ref. 3). A comparison of these factors with those obtained for a velocity-profile exponent of 1/7 is made in figure 5. The experimental values of H_{tot}, P_{tot}, and E_{tot} conformed closely with the theoretical factors for $n = 1/7$ over the velocity range studied. Thus it appears that for this blade row, the average form factor and the loss factors can be approximated by a simple-power-law velocity profile having an exponent of 1/7.

Blade-Surface Characteristics

Momentum loss. - The boundary-layer characteristics were also obtained on each surface of the stator blade using the minimum total-pressure point on the traces as the demarcation point between the two surfaces (fig. 2). The ratio of momentum thickness to chord as computed for the two surfaces is shown in figure 6 as a function of the blade-outlet critical-velocity ratio $(V/V_{cr})_{0,2}$. On the suction surface, a general reduction in (θ_s/c) occurs with increasing velocity. On the pressure surface, a more gradual reduction in (θ_p/c) occurs, except for the point at critical-velocity ratio of 1.16. Thus the trends of momentum loss obtained for the two blade surfaces are similar to that obtained for the blade. It can be seen from figure 6 that the momentum loss for the suction surface is approximately 2 to $2\frac{1}{2}$ times as great as the loss for the pressure surface.

Form and loss factors. - The form factors, energy factors, and pressure factors are shown for the two surfaces in figure 7. Included on the figure are the curves of H, E, and P for a simple-power-law velocity profile having an exponent of 1/7. These form and energy factors obtained experimentally are closely approximated by the values obtained from a simple-power-law velocity profile having an exponent of 1/7 over

the velocity range. The pressure factor obtained for the pressure sur-
face agrees closely with the $n = 1/7$ exponent curve. The pressure
factors obtained on the suction surface approach an exponent of 1/5 at
the high velocities. However, this deviation is not large, the maximum
deviation being of the. order of 6 percent. It is therefore believed
that the simple power-law velocity profile having an exponent of 1/7 can
be used to approximate the parameters H, P, and E with only a slight
error for the two surfaces as well as for the blade as a whole.

Comparison of Experimental and Theoretical Results

Total momentum loss. - The momentum-thickness-to-chord ratios are
replotted in figure 8(a) as a function of the blade-outlet critical-
velocity ratio. Included in the figure is a dashed line based on the
theoretical results obtained at $(V/V_{cr})_{0,2}$ values of 0.5, 0.75, 1.00,
and 1.46. As can be seen from the figure, the theoretical curve agrees
reasonably well with the experimental values over the range of blade-
outlet velocity, the theoretical values being slightly lower.

In obtaining the theoretical value of (θ_{tot}/c) at limiting load-
ing, no shock losses were assumed. Actually there would be some shock
losses extending across the free-stream flow at this velocity level,
and the shock would thicken the boundary layer, as well as negate the
assumption of isentropic free-stream flow employed. The value of
(θ_{tot}/c) at limiting loading was used as a guide in extending the theo-
retical curve from a $(V/V_{cr})_{0,2}$ value of 1.0 to 1.16. In addition,
the theoretical values are affected by the accuracy of obtaining the
velocity distribution. The velocity distributions were obtained by
stream filament theory, which, at best, can only be regarded as a good
approximation.

The trend of decreasing $(\theta_{tot}/c)_2$ with increasing $(V/V_{cr})_{0,2}$ can
be noted in figure 8(a) for the theoretical curve. This trend is due
partly to Reynolds and Mach number effects. From the theoretical equa-
tion for the boundary-layer momentum thickness it can be shown that
θ/c is proportional to $(\rho V c/\mu)_0^{-0.211}$ and $(T/T')_0^{0.368}$. The trend of
the experimental points was similar to that of the theoretical curve
over the range of outlet velocity. This result substantiates to some
degree the effect of Mach and Reynolds numbers that was assumed in the
theory.

Blade-surface momentum loss. - The boundary-layer momentum-thickness-
to-chord ratios obtained on the suction and pressure surfaces are com-
pared in figure 8(b) with the theoretical values. The agreement between

3949

the theoretical and experimental values is reasonably good over the range of outlet velocity. The theoretical values are similar in trend to the experimental points. It can be seen in figure 8(b) that the theoretical method also provides a reasonably good estimation of the breakdown of loss between the two surfaces.

SUMMARY OF RESULTS

The blade-outlet boundary-layer characteristics at the mean radius of a typical turbine stator blade have been obtained experimentally over a range of blade-outlet critical-velocity ratios from 0.8 to 1.16. The total boundary-layer momentum thickness and the momentum thicknesses obtained on each surface were compared with the values calculated from the turbulent-boundary-layer theory. The boundary-layer form, pressure, and energy factors for the blade, as well as for the two surfaces, were compared with the values obtained for a simple-power-law velocity profile having an exponent of 1/7. The results were as follows:

1. The theoretical values of the boundary-layer momentum thickness for the blade and for the two surfaces individually were reasonably close to the experimental values, the theoretical values being slightly lower.

2. The theoretical curve of boundary-layer momentum thickness as a function of blade-outlet critical-velocity ratio was similar in trend to that of the experimental points. This result indicated that the boundary-layer thickness was affected by Reynolds and Mach numbers substantially in the manner assumed in the theory.

3. The boundary-layer form factor, pressure factor, and energy factor for the two surfaces, as well as the average values for the blade, could be satisfactorily approximated by a simple-power-law velocity profile having an exponent of 1/7.

Lewis Flight Propulsion Laboratory
    National Advisory Committee for Aeronautics
        Cleveland, Ohio, November 25, 1955

APPENDIX A

SYMBOLS

C_{fr} skin-friction coefficient, dimensionless

c blade chord, ft

D demarcation point on total-pressure traces (fig. 2)

d distance from boundary of total-pressure trace to demarcation
point D, ft

E energy factor, ψ/θ; $E = \psi^*/\theta^*$

g acceleration due to gravity, 32.17 ft/sec^2

H form factor, δ/θ; $H = \delta^*/\theta^*$

H_{inc} incompressible-flow form factor for simple power-law velocity
profile, $2n + 1$

K compressibility correction factor, $\left[1 - \dfrac{\gamma - 1}{\gamma + 1}\left(\dfrac{V}{V_{cr}}\right)_0^2\right]^{0.467}$

n exponent used to describe simple boundary-layer velocity profile;
$(V/V_0) = (y/\delta_f)^n$

P pressure factor, ξ/θ; $P = \xi^*/\theta^*$

p pressure, lb/sq ft

Re Reynolds number

Re_θ Reynolds number based on boundary-layer momentum thickness

s blade spacing or pitch, ft

T temperature, $^\circ R$

t blade trailing-edge thickness, ft

u distance along circumferential path, ft

V   gas velocity, ft/sec

x   distance along blade surface measured from forward stagnation
         point, ft

y   distance normal to blade surface, ft

β blade-outlet flow angle measured from axial direction, deg

γ ratio of specific heats

δ boundary-layer displacement thickness, ft

δ_f full boundary-layer thickness, ft

δ_{te} ratio of projection of trailing-edge thickness along circum-
         ferential path to blade pitch, $t/(s \cos \beta)$

δ^* displacement-thickness parameter, $\delta/(s \cos \beta)$

θ boundary-layer momentum thickness, ft

θ^* momentum-thickness parameter[1], $\theta/(s \cos \beta)$

μ gas viscosity, lb/(ft)(sec)

ξ boundary-layer pressure thickness, ft

ξ^* pressure-thickness parameter, $\xi/(s \cos \beta)$

ρ gas density, lb/cu ft

τ wall shearing stress, lb/sq ft

ψ boundary-layer energy thickness, ft

ψ^* energy-thickness parameter, $\psi/(s \cos \beta)$

Subscripts:

c   compressible flow

cr   conditions at Mach number of 1.0

---

[1]Relations among the various momentum-thickness parameters θ_{tot},
θ_s, θ_p, θ_{tot}^*, θ_s^*, and θ_p^* are shown schematically in figure 2. The re-
lations among the various forms of the other thickness parameters δ,
ψ, and ξ used herein are similar.

inc   incompressible flow

p   pressure surface

s   suction surface

tot   sum of pressure- and suction-surface quantities

x   referring to any particular value of x

0   conditions at free stream outside boundary layer

1   blade-inlet

2   blade-outlet

Superscripts:

'   total state

APPENDIX B

INTEGRATION OF THEORETICAL BOUNDARY-LAYER MOMENTUM-THICKNESS EQUATION

Combining the two equations for τ (eqs. (3) and (4)) and including the compressibility factor K give the following equation:

$$\frac{d(\rho_0 V_0^2 \theta)}{dx} + \frac{\rho_0 V_0 \delta dV_0}{dx} = \frac{\rho_0 V_0^2}{2} \frac{0.246 \, K}{(Re_\theta)^{0.268}(10)^{0.678(2n+1)}} \tag{B1}$$

After multiplication by dx, and substitution of $H\theta$ for δ, equation (B1) may be written as

$$V_0^2 \theta \, d\rho_0 + \rho_0 V_0^2 \, d\theta + 2\rho_0 V_0 \, \theta \, dV_0 + \rho_0 V_0 H\theta \, dV_0 =$$

$$\left[\frac{0.123 \rho_0 V_0^2}{10^{0.678(2n+1)}} \left(\frac{\rho_0 V_0 \theta}{\mu_0} \right)^{-0.268} K \right] dx \tag{B2}$$

Multiplying equation (B2) by V_0^H and $\left[\rho_0 V_0^{(2+H)} \theta \right]^{0.268}$ yields

$$\left[\rho_0 V_0^{(2+H)} \theta \right]^{0.268} \left[V_0^{(2+H)} \theta \, d\rho_0 + \rho_0 V_0^{(2+H)} d\theta + (2 + H)\rho_0 \theta \, V_0^{(1+H)} dV_0 \right] =$$

$$\left\{ \frac{0.123 \left[\rho_0 V_0^{(2+H)} \right]^{1.268}}{10^{0.678(2n+1)}} \left(\frac{\mu}{\rho V} \right)_0^{0.268} K \right\} dx \tag{B3a}$$

or

$$\left[\rho_0 V_0^{(2+H)} \theta \right]^{0.268} d\left[\rho_0 V_0^{(2+H)} \theta \right] = \left\{ \frac{0.123 \left[\rho_0 V_0^{(2+H)} \right]^{1.268} \left(\frac{\mu}{\rho V} \right)_0^{0.268}}{10^{0.678(2n+1)}} K \right\} dx \tag{B3b}$$

This equation is now integrable as follows:

$$\frac{1}{1.268} \left[\rho_0 V_0^{(2+H)} \theta \right]_x^{1.268} = \int_0^x \frac{0.123}{10^{0.678(2n+1)}} \left[\rho_0 V_0^{(2+H)} \right]^{1.268} \left(\frac{\mu}{\rho V} \right)_0^{0.268} K \cdot dx \tag{B4}$$

or

$$\theta_x^{1.268} = \frac{0.156}{\left[\rho_0 V_0^{(2+H)}\right]_x^{1.268}} \int_0^x \frac{\left[\rho_0 V_0^{(2+H)}\right]^{1.268}\left(\frac{\mu}{\rho V}\right)_0^{0.268}}{10^{0.678(2n+1)}} K \cdot dx \qquad (B5)$$

Raising both sides of equation (B5) to the 1/1.268 power and dividing numerator and denominator by ρ_0' and $V_{cr,0}^{(2+H)}$ gives

$$\theta_x =$$

$$\frac{0.231}{\left[\left(\frac{\rho V}{\rho' V_{cr}}\right)_0\left(\frac{V}{V_{cr}}\right)_0^{(1+H)}\right]_x}\left\{\int_0^x \frac{\left[\left(\frac{\rho V}{\rho' V_{cr}}\right)_0\left(\frac{V}{V_{cr}}\right)_0^{(1+H)}\right]^{1.268}\left(\frac{\mu}{\rho V}\right)_0^{0.268} K \cdot dx}{10^{0.678(2n+1)}}\right\}^{0.7886}$$

$$(6)$$

REFERENCES

1. Schlichting, H.: Lecture Series "Boundary Layer Theory." Pt. I - Laminar Flows. NACA TM 1217, 1949.

2. Schlichting, H.: Lecture Series "Boundary Layer Theory." Pt. II - Turbulent Flows. NACA TM 1218, 1949.

3. Stewart, Warner L.: Analysis of Two-Dimensional Compressible-Flow Loss Characteristics Downstream of Turbomachine Blade Rows in Terms of Basic Boundary-Layer Characteristics. NACA TN 3515, 1955.

4. Huppert, Merle C., and MacGregor, Charles: Comparison Between Predicted and Observed Performance of Gas-Turbine Stator Blade Designed for Free-Vortex Flow. NACA TN 1810, 1949.

5. Goldstein, Sydney, ed.: Modern Developments in Fluid Dynamics. Vol. I. Clarendon Press (Oxford), 1938, pp. 131-134.

6. Ludwieg, H., and Tillmann, W.: Investigations of the Wall-Shearing Stress in Turbulent Boundary Layers. NACA TM 1285, 1950.

3949

7. Rubesin, Morris W., Maydew, Randall C., and Varga, Stephen A.: An Analytical and Experimental Investigation of the Skin Friction of the Turbulent Boundary Layer on a Flat Plate at Supersonic Speeds. NACA TN 2305, 1951.

8. Tucker, Maurice: Approximate Turbulent Boundary-Layer Development in Plane Compressible Flow Along Thermally Insulated Surfaces with Application to Supersonic-Tunnel Contour Correction. NACA TN 2045, 1950.
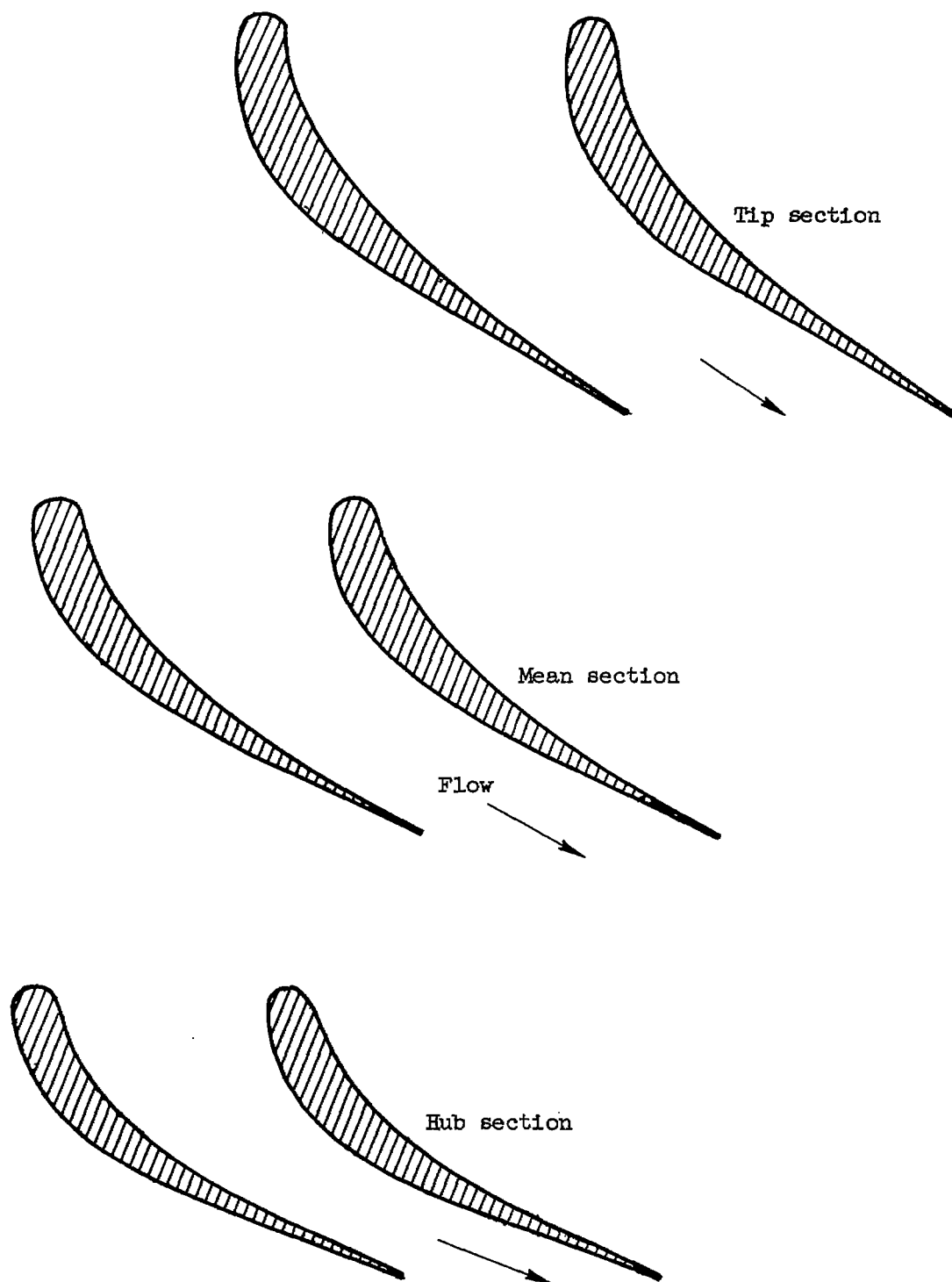
3949

Tip section

Mean section

Flow

Hub section

Figure 1. - Stator-blade passages and profiles.

(a) Blade-outlet critical-velocity ratio, $(V/V_{cr})_{0,2}$, 0.831.

(b) Blade-outlet critical-velocity ratio, $(V/V_{cr})_{0,2}$, 0.877.

(c) Blade-outlet critical-velocity ratio, $(V/V_{cr})_{0,2}$, 0.939.

$$\frac{a}{s} = \theta_s^* \qquad \frac{e}{s} = \delta_{te}$$

$$\frac{b}{s} = \theta_p^* \qquad \theta_s + \theta_p = \theta_{tot}$$

$$\frac{a+b}{s} = \theta_{tot}^*$$

Sketch of boundary-layer momentum parameters.
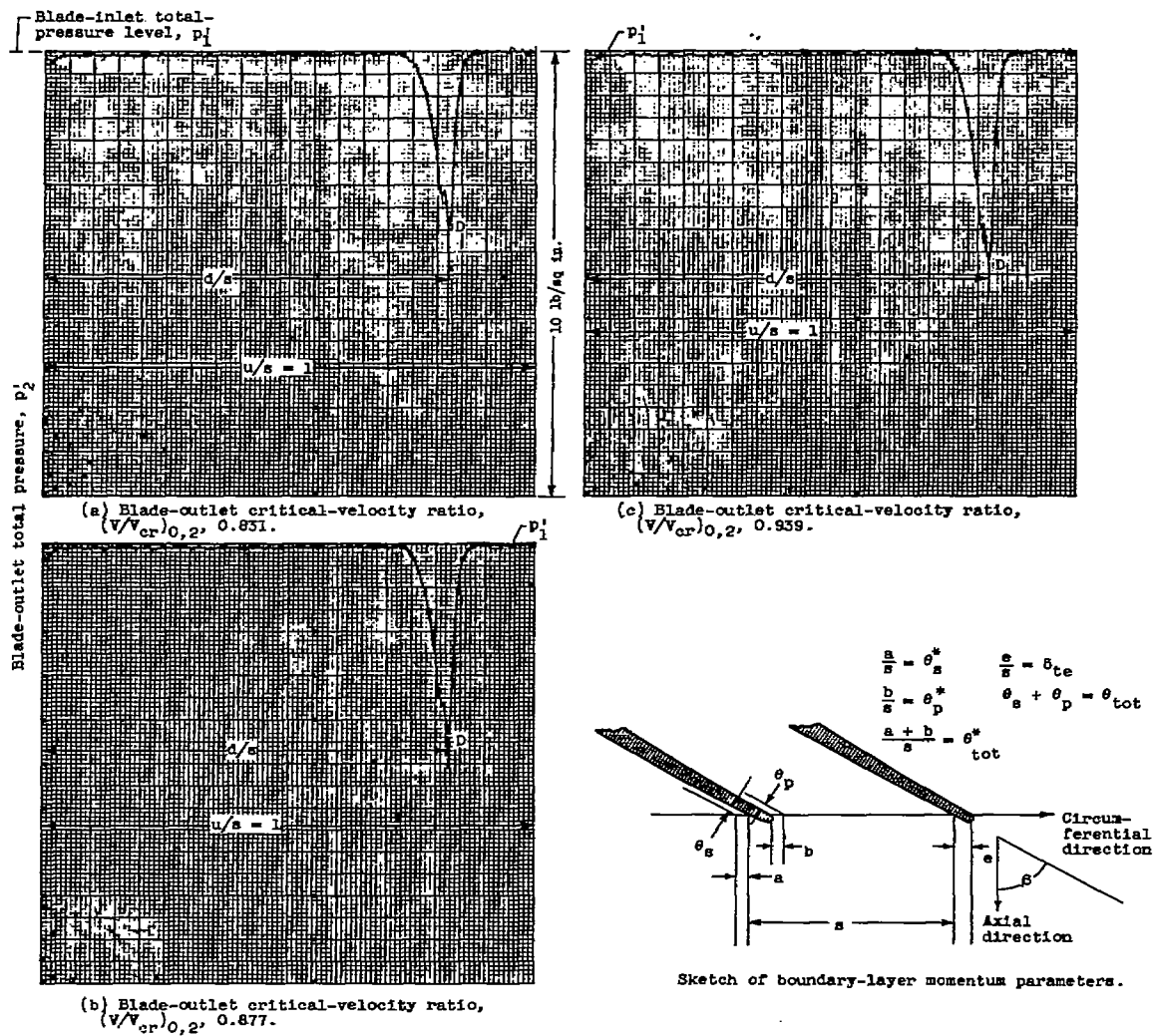
Figure 2. - Blade-outlet total-pressure traces and sketch showing relations among various momentum-thickness parameters. Blade-inlet total pressure, p_1', 31.99±0.03 inches of mercury.
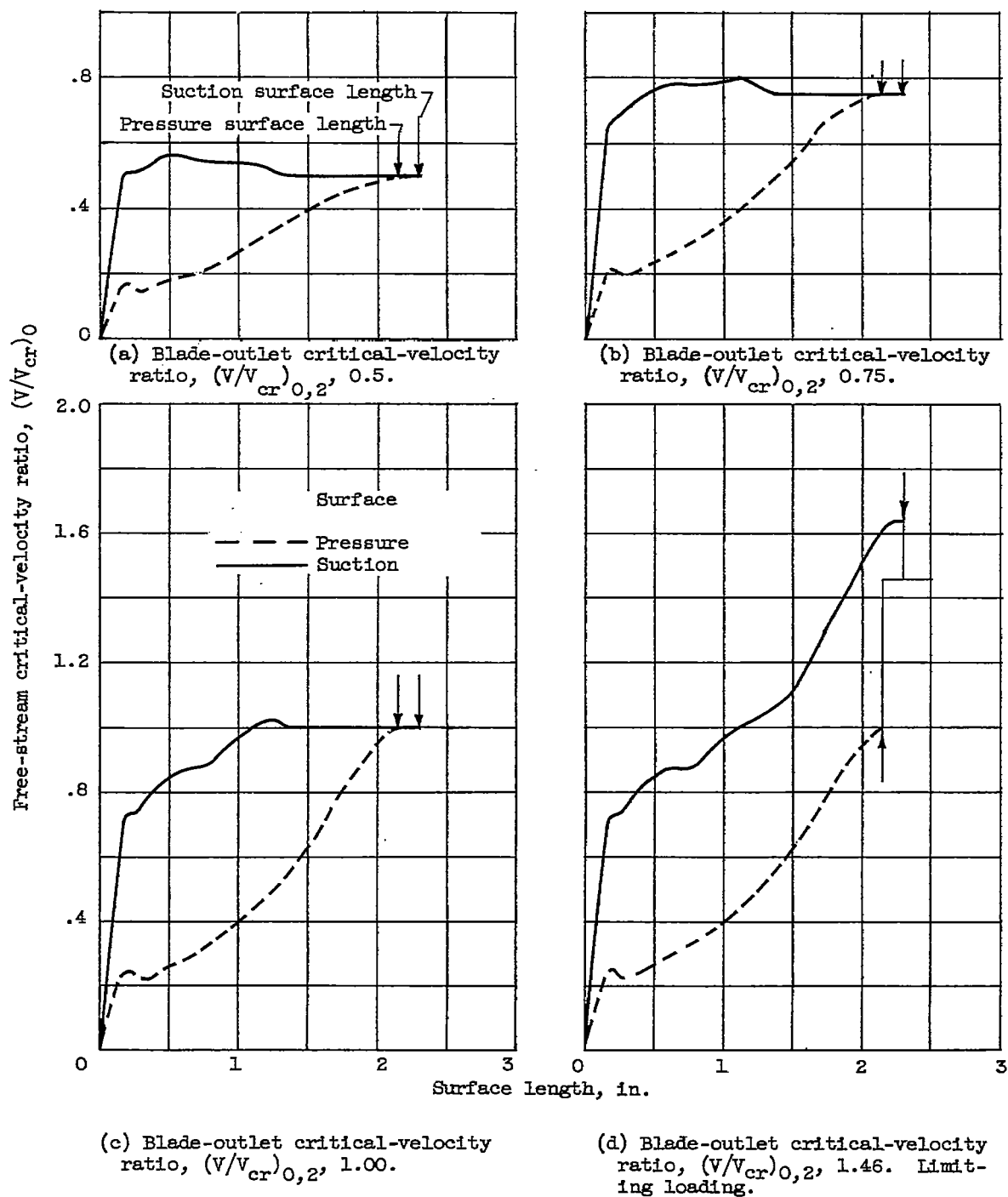
(d) Blade-outlet critical-velocity ratio, $(V/V_{cr})_{0,2}$, 1.04.

(f) Blade-outlet critical-velocity ratio, $(V/V_{cr})_{0,2}$, 1.24.

(e) Blade-outlet critical-velocity ratio, $(V/V_{cr})_{0,2}$, 1.15.

(g) Blade-outlet critical-velocity ratio, $(V/V_{cr})_{0,2}$, 1.40.
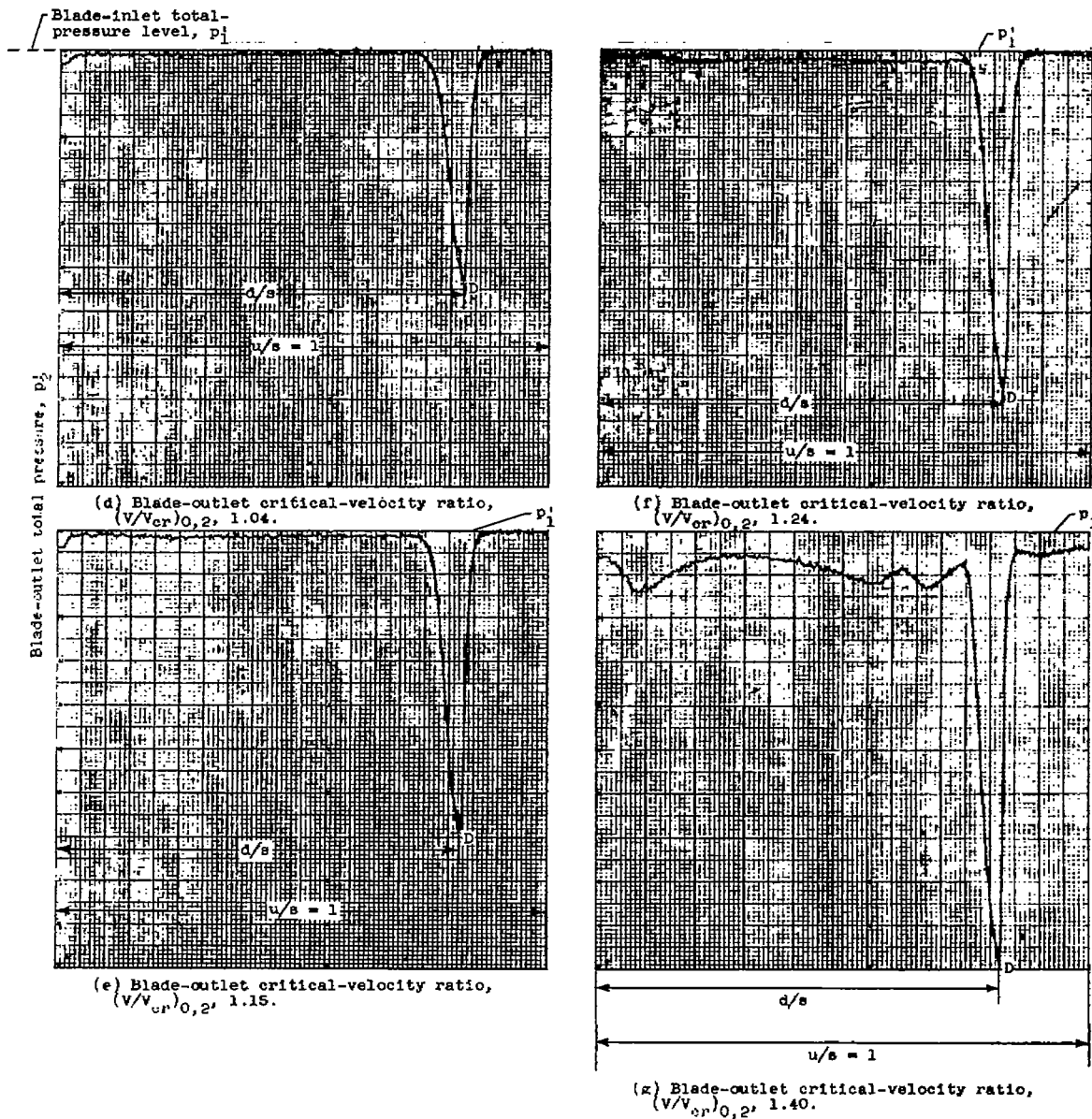
Figure 2. - Concluded. Blade-outlet total-pressure traces and sketch showing relation of various momentum-thickness parameters. Blade-inlet total pressure, p_1', 31.99±0.03 inches of mercury.

CK-3 back

(a) Blade-outlet critical-velocity ratio, $(V/V_{cr})_{0,2}$, 0.5.

(b) Blade-outlet critical-velocity ratio, $(V/V_{cr})_{0,2}$, 0.75.

(c) Blade-outlet critical-velocity ratio, $(V/V_{cr})_{0,2}$, 1.00.

(d) Blade-outlet critical-velocity ratio, $(V/V_{cr})_{0,2}$, 1.46. Limiting loading.

Figure 3. - Velocity distributions obtained from stream filament theory for various critical-velocity ratios.
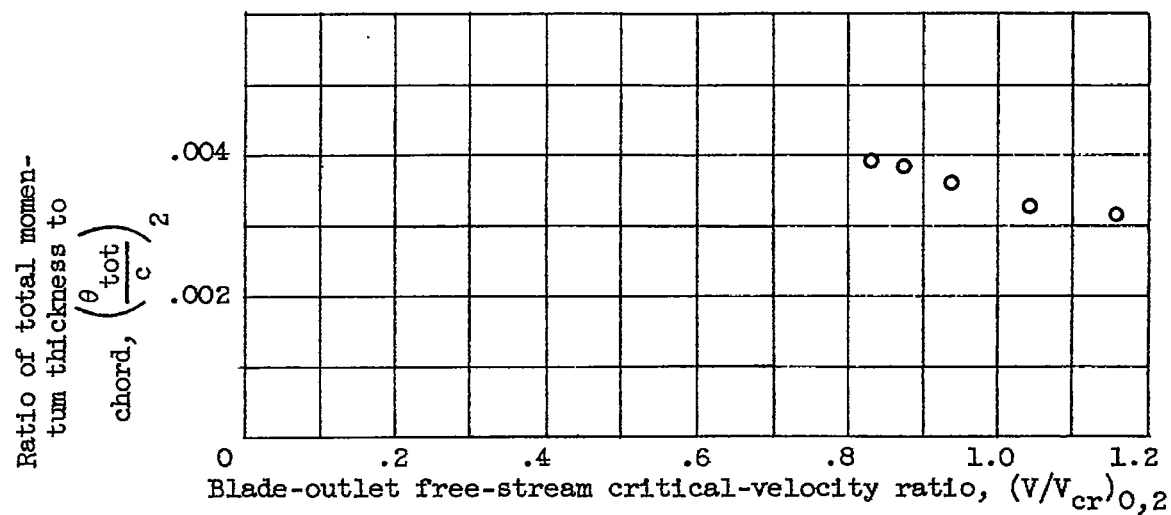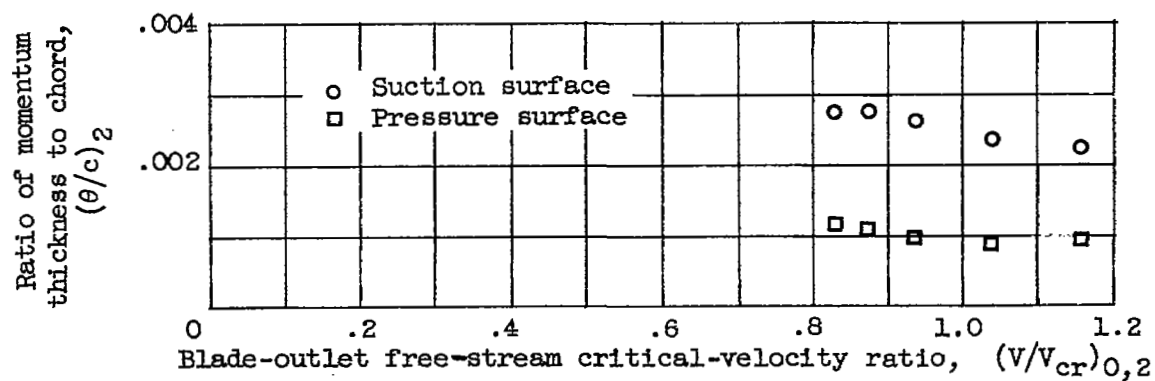
Figure 4. - Ratio of total momentum thickness to chord as function of blade-outlet free-stream critical-velocity ratio at stator mean section.
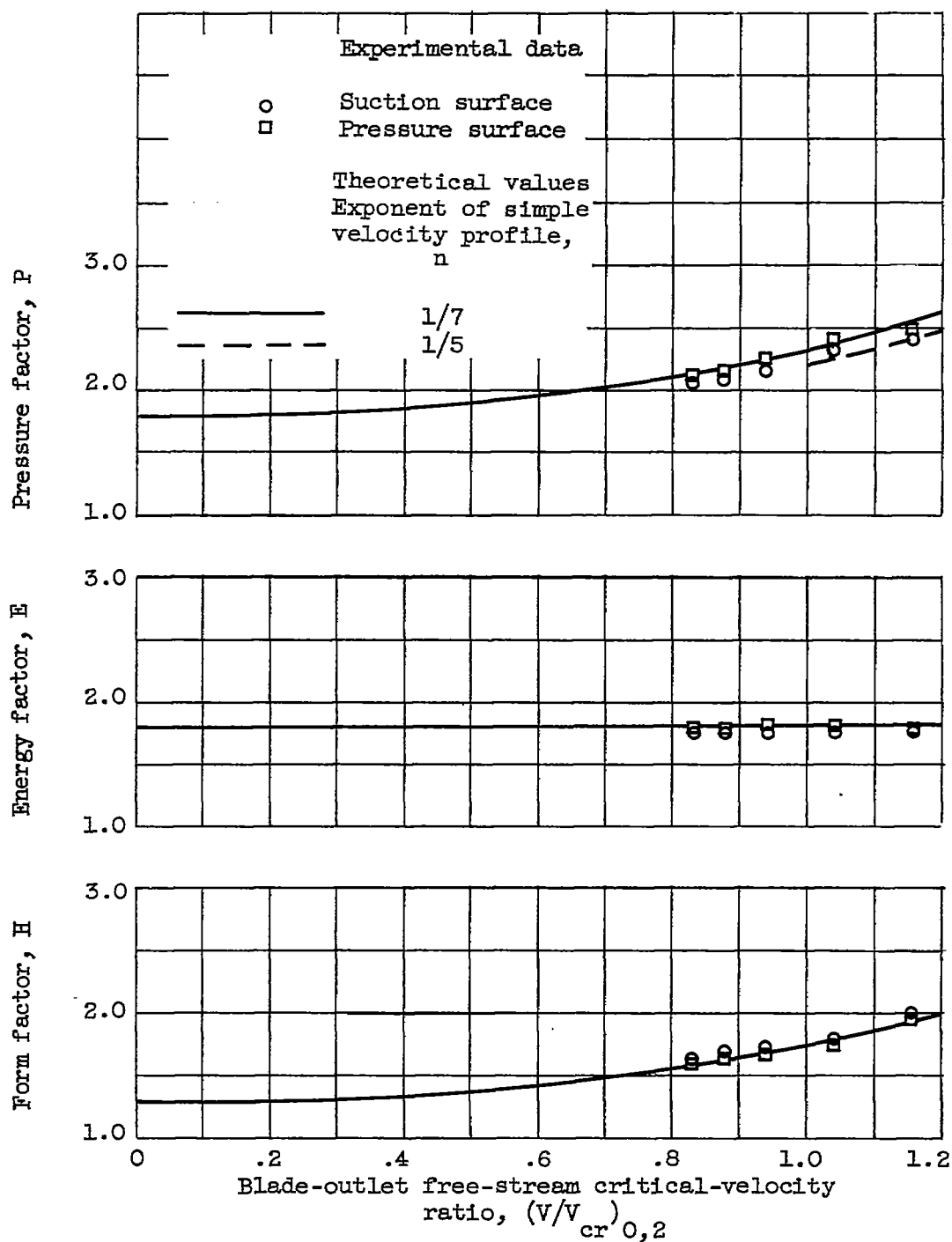
3949
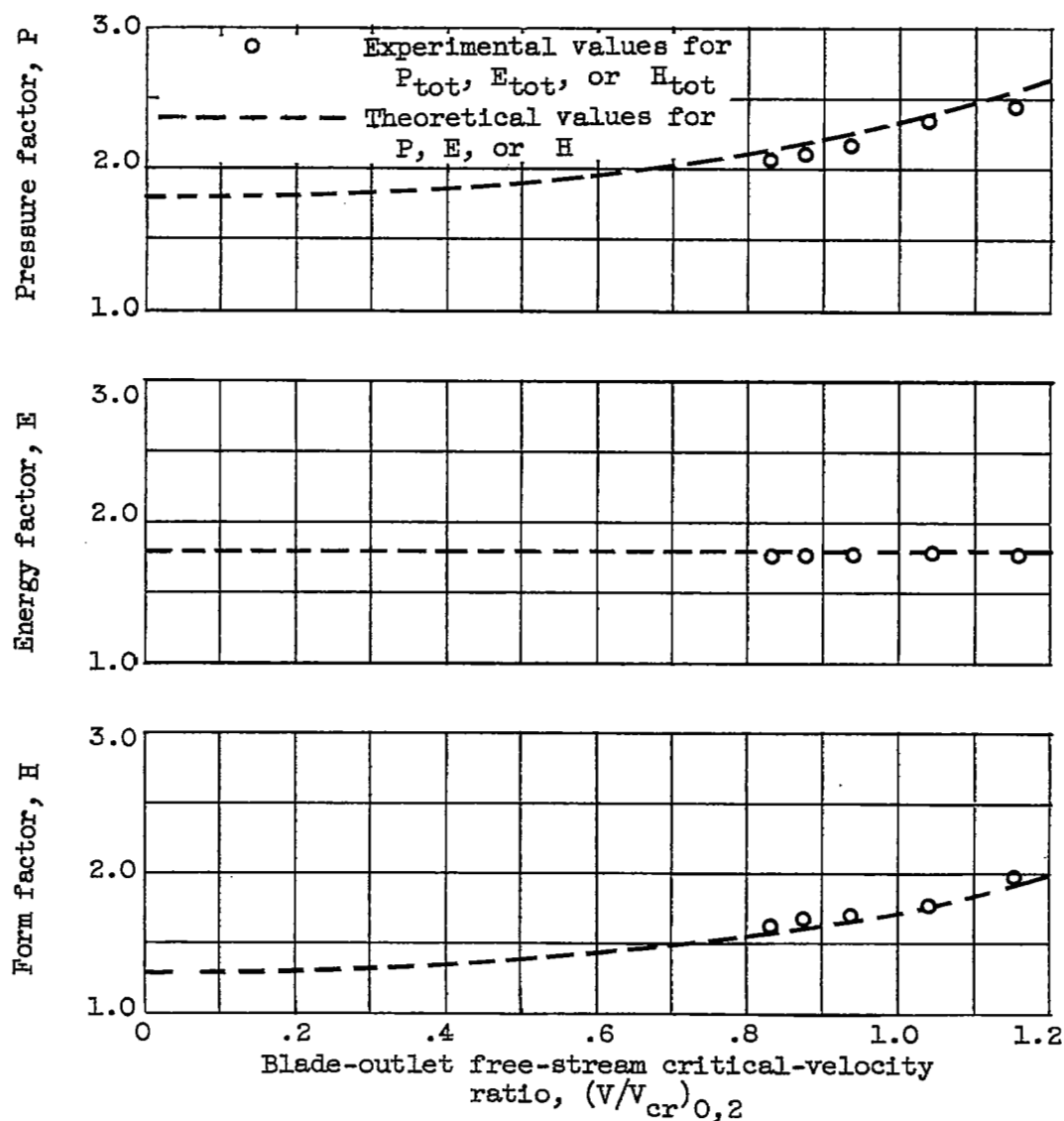
Figure 5. - Variation in boundary-layer factors with
blade-outlet free-stream critical-velocity ratio.
Simple-velocity-profile exponent for theoretical
values, n, 1/7.

Figure 6. - Ratio of total momentum thickness to chord as
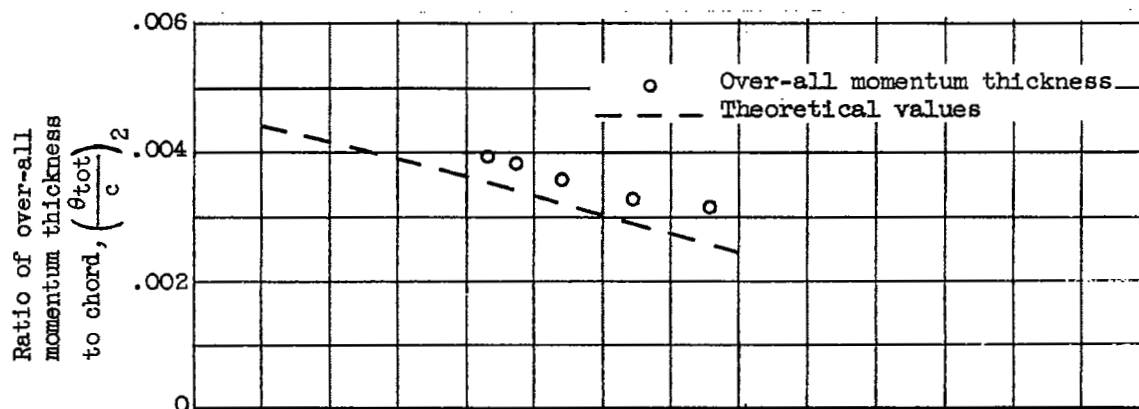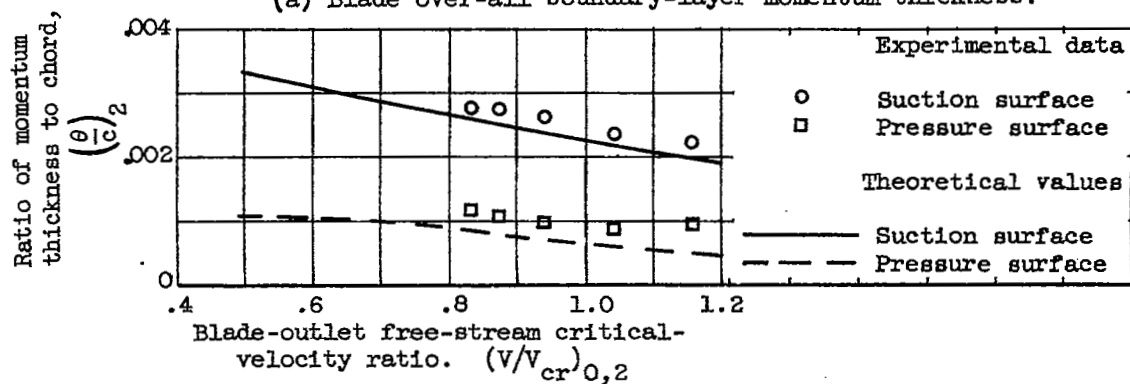function of blade-outlet free-stream critical-velocity
ratio at stator mean section.

3949

Figure 7. - Variation in surface boundary-layer factors with blade-outlet free-stream critical-velocity ratio.

3949

(a) Blade over-all boundary-layer momentum thickness.

(b) Boundary-layer momentum thickness of suction and pressure surfaces.

Figure 8. - Comparison of theoretical and experimental boundary-layer momentum thicknesses.